**ORIGINAL ARTICLE**

# Experimental study of pulse detonation engine with liquid ethanol and oxygen mixtures

**H. Kadosh**[1] · **D. Michaels**[1]

**Abstract**

Pulse detonation engine burns fuel and oxidizer using detonation waves. As in other volume-limited propulsion devices, the use of liquid fuel in a pulse detonation engine is preferred. An experimental study of a pulse detonation engine with liquid ethanol fuel and oxygen mixture was carried out. The research of detonation in ethanol was limited to gaseous mixtures only, and to the best of our knowledge, this is the first published data on detonation in a heterogeneous liquid ethanol and oxygen mixture. Single-cycle tests were made with several engine lengths (45–75 cm) and diameters (6–15 mm), a variety of equivalence ratios, and different deflagration-to-detonation (DDT) enhancement methods. A two-fluid atomizer was used for ethanol injection, and the droplet size distribution was measured. The heterogeneous stoichiometric mixture had a Sauter mean diameter of 30 μm at the exit of the atomizer, and the droplet size distribution shifted toward a larger diameter for higher equivalence ratios and downstream along the tube. A fully developed detonation was observed at and above 60-cm-long smooth tube. A maximum velocity deficit of 400 m/s relative to the theoretical Chapman–Jouguet detonation velocity for the gaseous ethanol–oxygen mixture was measured. A weak ignition source of 1.1 mJ and DDT enhancement methods were demonstrated. Shchelkin spirals and grooved insert, with blockage ratio of 53% and 51%, respectively, were tested. A 15-cm grooved insert enabled a decrease in the required detonation tube length from 60 cm to 45 cm, whereas the Shchelkin spiral showed a significantly lower effect.

**Keywords** Pulse detonation engine · Ethanol · Liquid fuel · Heterogeneous mixture · Deflagration to detonation transition

## 1 Introduction

Pulse detonation engine (PDE) burns fuel and oxidizer using detonation waves. The engine consists of a tube closed at one end and open at the other. Fuel and oxidizer are injected near the head end, and the mixture is ignited. Following a deflagration-to-detonation process, the detonation travels toward the open end of the tube, leaving behind a high-pressure and high-temperature gas that generates thrust as it expands and leaves the tube [1]. Pulse detonation engines have been attracting considerable attention because they promise performance improvements over existing air-

breathing or rocket propulsion devices [2]. The near-constant volume operational cycle of PDE provides a higher thermodynamic efficiency compared to the constant-pressure (Brayton) cycle. The advantages of pulse detonation engines are reduced fuel consumption and capability of operation from zero to high velocity [3].

Airborne applications are volume limited; therefore, the use of liquid fuel in PDE is preferred [4]. Research about heterogeneous mixture detonation began 60 years ago. Dabora et al. [5,6] experimentally studied detonations in diethylcyclohexane ($C_{10}H_{20}$) and gaseous oxygen mixtures and observed a velocity deficit relative to the theoretical Chapman–Jouguet (CJ) detonation velocity that was linked to the reaction length and droplet breakup time. Gubin et al. [7] suggested that the velocity deficit is due to incomplete fuel reaction and that the detonation velocity approaches the CJ velocity for droplets smaller than 20 μm. Brophy et al. [8,9] demonstrated the use of liquid aviation fuel in pulse detonation engines. They initiated detonations in JP-10-$O_2$ mixtures with droplets diameter below 10 μm. The

Communicated by E. Gutmark.

✉ H. Kadosh
  khertzel@campus.technion.ac.il

  D. Michaels
  danm@technion.ac.il

1  Faculty of Aerospace Engineering, Technion – Israel Institute of Technology, Haifa, Israel

observation made is that in two-phase flow, the fuel must be significantly vaporized for detonation to propagate. They reported that very fine aerosols were required to support detonation in JP-10-air mixtures and that longer ignition delay time improved the mixing of fuel vapor. Frolov et al. [10] have optimized the detonation initiation by electric discharges of a mixture of n-hexane and air. They concluded that for minimal energy requirement, two igniters to be used, one located at the tube head end and the other located downstream to be triggered in-phase with primary shock wave arrival. They further decreased the initiation energy of the detonation by using a Shchelkin spiral and a tube coil.

Bar-Or et al. [11] obtained different behaviors of fuels with low vapor pressure (decane and kerosene) and high vapor pressure (heptane), both with the same monodisperse droplets clouds of $400\,\mu$m. In the case of low vapor pressure, long reaction zones and propagation rates below CJ velocity were observed. In the high-vapor-pressure case, a gaseous detonation was observed to propagate through the fuel vapor already present followed by an extended region of droplet burning.

During recent years, there has been increased interest in the use of ethanol as a renewable fuel for automotive and power generation applications [12]. Ethanol ($C_2H_5OH$) is liquid at room temperature and has a high vapor pressure of 5.95 kPa at 293 K (relative to 0.4 kPa of JP-10 at the same temperature). That has raised our interest in the usage of ethanol as a fuel candidate for pulse detonation engines.

Research of detonation in ethanol was mainly motivated by safety reasons. Diakow et al. and Mendiburu et al. [12,13] measured the detonation cell structure of ethanol and dimethyl ether (DME) vapor–air mixtures at atmospheric pressure and compared it to the calculated one-dimensional detonation reaction zone length. The detonation cell size for stoichiometric ethanol–air mixture at 303 K was found to be in the range of 30–40 mm. Mendiburu et al. [13] studied the flame acceleration and deflagration-to-detonation transition in ethanol–air mixtures in a tube filled with orifice plates. They reported that for mixtures at initial pressure of 101 kPa and both initial temperatures of 373 K and 473 K, the detonation was limited to equivalence ratio ($\phi$) of 1.1–1.3, whereas mixtures at lower initial pressure of 60 kPa did not result in DDT. Ng et al. [14] took measurements of the detonation velocities and characteristic cell sizes in DME–oxygen mixtures. Detonation cell sizes estimated using a correlation model by Ng et al. [15,16] were in good agreement with their results and order of magnitude smaller than that of Diakow et al. [12] which has used air instead of oxygen.

The research of detonation in ethanol–air, DME–air, and DME–oxygen was limited to gaseous mixtures only, and to our best knowledge, there is no published information on detonation in a liquid (or gaseous) ethanol–gaseous oxygen mixture related to pulse detonation engine. The research objective is the characterization of detonation development in liquid ethanol and oxygen mixtures within an acceptable engine length and with a weak ignition source (an order of a few millijoules per discharge) and with the assist of enhancement methods as Shchelkin spiral or grooved insert.

## 2 Experimental setup

A modular pulse detonation engine was designed, and the schematics of the experimental setup are shown in Figs. 1 and 2. The engine was made of multiple stainless-steel 15-cm-long flange sections, with an inner diameter ($D$) of 6, 10, and 15 mm. The overall engine length ($L$) was varied between 45 and 75 cm. The liquid ethanol and gaseous oxygen were supplied by an atomizer located on the engine head end. The fuel flow rate was controlled by a pressure controller (Alicat PCD-500PSIG-D), that was designed to set a nitrogen pressure inside the fuel cylinder, and a Coriolis flow meter (Bronkhorst M14) in order to reduce measurement uncertainties. The fuel flow rate was initially calibrated with pressure for the required range of flow rate. A constant oxygen flow rate (2.7 g/s) was monitored by an orifice flow meter (Alicat M-250SLPM-D). Both liquid ethanol and oxygen supply was controlled by solenoid valves with a response time of 0.5 to 3 ms.

Two spark plugs (Rcexl A-02) were placed 10 mm downstream the atomizer. The average spark energy of the ignition source was initially measured and found to be 1.1 mJ, with a peak voltage of 4.4 kV and a peak current of 0.7 A. The ignition started once the ethanol and oxygen supply was completed and the solenoid valves were closed.

Two piezoelectric pressure transducers (PCB 113B24), with a response time of 1 $\mu$s, were used to measure the detonation wave pressure rise. To fully realize the high-frequency response time of the transducers, they were flush-mounted [17]. The pressure transducers were placed 10 mm from the engine open end, 413 mm from the igniters (for 45-cm-long engine), and 40 mm apart. The sampling rate was 1 MHz, and the sampling period was 3 s. Purged nitrogen was used to cool down the engine between subsequent experiments and maintain the pressure transducers within their temperature limits.

A data acquisition and analysis interface was built, and the engine was controlled and monitored from it. An example of the control signals for the fuel and oxygen valves and the spark plugs is shown in Fig. 3. The signal length for the fuel and oxygen valves was a result of the combustion chamber volume and the fuel and oxygen flow rate. The ignition signal was given after the fuel and oxygen valves were closed and taking into account their response time.

The PDE was operated with a frequency of 1 Hz and a period of 3 s (three pulses). The low frequency prevented
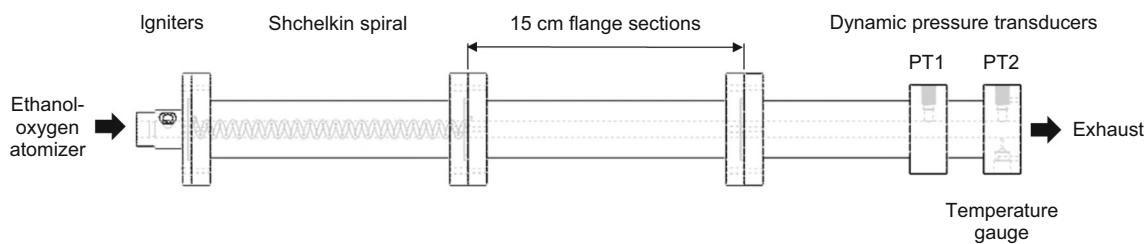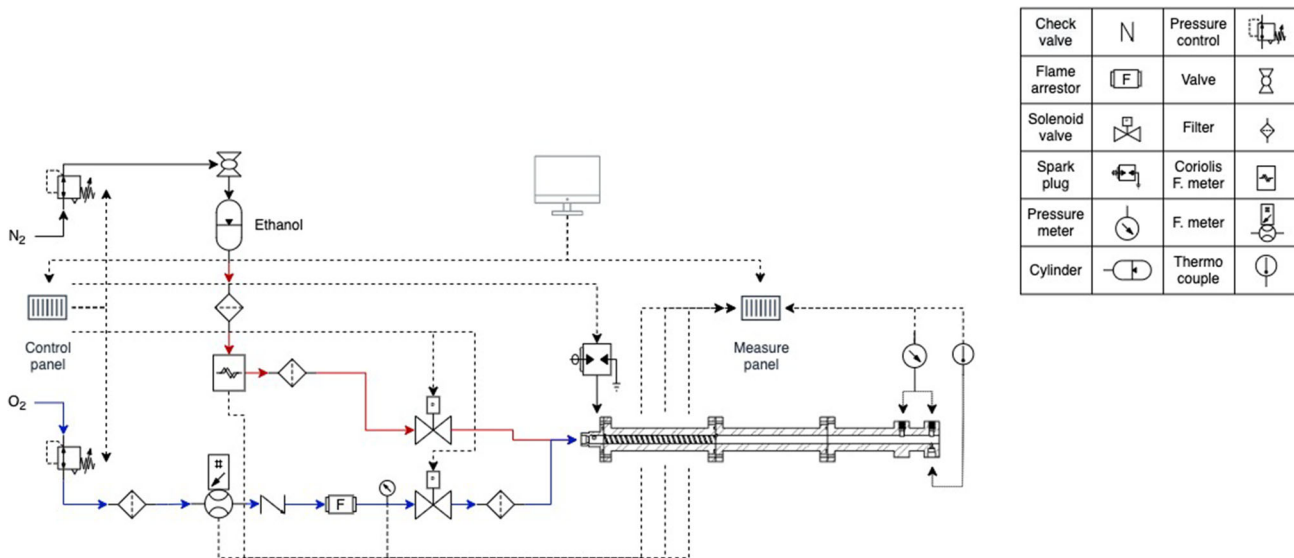
**Fig. 1** Pulse detonation engine schematic


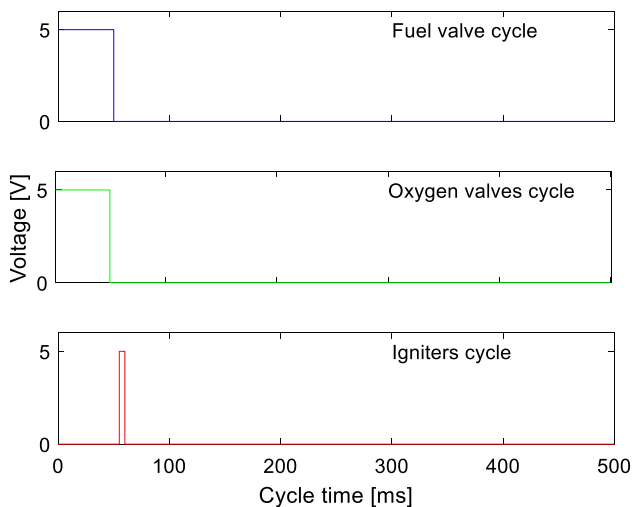
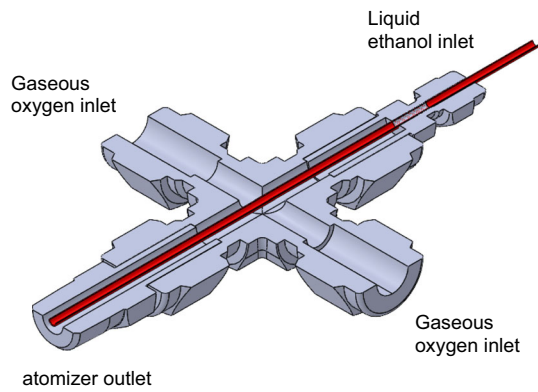**Fig. 2** The experiment setup of a pulse detonation engine



**Fig. 3** A schematics of the control signals for the fuel and oxygen valves and the igniters (the cycle time is 1 s)

**Table 1** Summary of experiment parameters

| Parameter | Values |
| --- | --- |
| Total length (cm) | 45, 60, 75 |
| Inner diameter (mm) | 6, 10, 15 |
| Spiral length (mm) | 150, 200, 250, 300 |
| Groove length (mm) | 150 |
| Equivalence ratio | 0.7–2.0 |

ditions inside the engine were 298 K and 101 kPa (both were measured by the oxygen flow meter). The ratio of the engine combustion chamber volume filled with a detonable mixture relative to the total combustion chamber volume, known as fill fraction (ff), was two (overfilled with twice the combustion chamber volume). This way, a homogenous and continuous path of a reactive mixture to detonation propagation is assured. A summary of the experiment parameters is detailed in Table 1.

the coupling between the subsequent cycles. The experiments were conducted using various engine diameters and lengths, without and with DDT enhancements methods and for a variety of equivalence ratios. The mixture initial con-
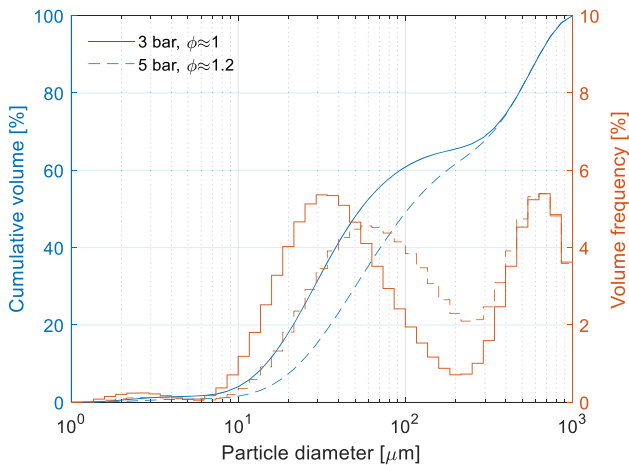
**Fig. 4** A cross section of a two-fluid oxygen-assisted atomizer



**Fig. 5** Ethanol droplet size distribution at 3 and 5 bar at 10 cm from the atomizer in open space



**Fig. 6** Ethanol droplet size distribution at 3 bar at the exit of the atomizer and the 60-cm tube



**Fig. 7** Ethanol SMD (as measured at the atomizer exit) versus fuel pressure at three different measurements



**Fig. 8** A cross section of a grooved insert with a BR of 51% inside a flange section
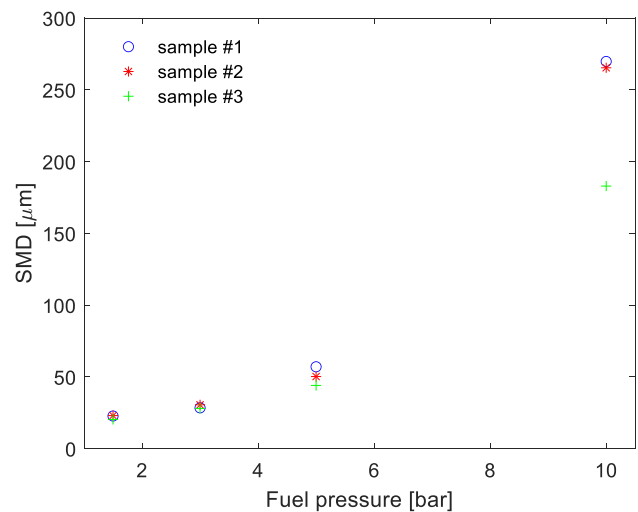
## 2.1 Atomization measurements

A two-fluid oxygen-assisted atomizer was used for ethanol injection. In general, breakup in a two-fluid atomizer is caused by the large relative velocity of the gaseous stream, which results in high deformation and instabilities on the liquid jet surface and breakup process. A section view of the atomizer in use is shown in Fig. 4. The atomizer is based on a union cross (Ham-Let 7102LSS1/4) fed from one inlet with liquid ethanol, through a 1/16-inch tube, and with gaseous oxygen from the two other perpendicular inlets. The pressure of the assist gaseous oxygen was set to 6.8 bar (limited by the oxygen solenoid valves), and the flow rate of the liquid ethanol was in the range of 0.9–2.6 g/s.
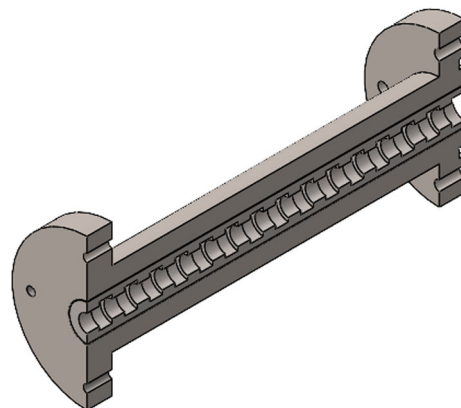
The size distribution of the ethanol droplet was measured in open space at the exit of the atomizer with a Malvern Spraytec laser diffraction system. The measurements were taken at an axial position of 10 cm from the atomizer and for fuel pressures 1.5, 3, 5, and 10 bar, which are equivalent to equivalence ratios of approximately 0.8, 1, 1.2, and 1.5, respectively. Another set of measurements were taken at an
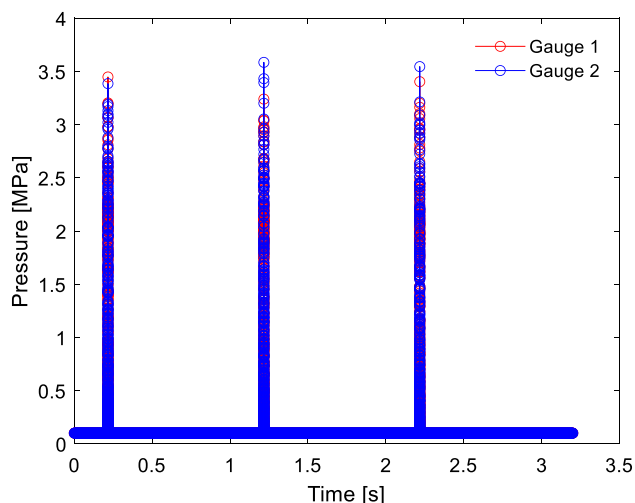
**Fig. 9** Pressure trace of a 3 s experiment, equivalence ratio $\phi = 1$
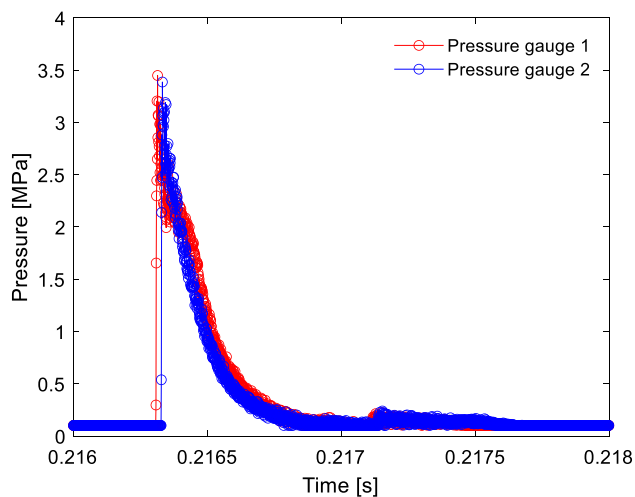


**Fig. 10** Detailed pressure trace, $\phi = 1$

axial position of 64 cm from the atomizer (4 cm downstream from the exit of the 60-cm tube) to estimate the effect of the tube on the spray. These measurements were taken for fuel pressures of 1.5 and 3 bar. The sampling rate was 1 kHz, and the measuring duration was 1 s with a trigger delay time of 500 ms. Three different samples were taken with 1000 measurements in each.

The spray cone angle was approximately 15°. The droplet size distributions at the exit of the atomizer for fuel pressures of 3 and 5 bar are shown in Fig. 5. The spray has a bimodal distribution with a higher volume of smaller droplets, and the droplet distribution shifted toward a larger diameter for higher pressures, as shown in Figs. 5 and 7.

A comparison of the droplet size distribution at a fuel pressure of 3 and 5 bar shows that at lower fuel pressure, a higher volume is occupied with small diameter droplets: approximately 31% cumulative volume of droplets with a

diameter smaller or equal to 30 μm at a fuel pressure of 3 bar and approximately 16% cumulative volume of droplets of the same diameter at a fuel pressure of 5 bar. The measured Sauter mean diameter (SMD, $d_{32}$) at equivalence ratio $\phi \approx 1$, for a fuel pressure of 3 bar, is nearly 30 μm and at $\phi \approx 1.2$, for a fuel pressure of 5 bar, is nearly 50 μm. An explanation for this observed trend can be related to the relative velocity of the two streams. As the fuel pressure increases, the fuel flow rate inside the atomizer increases, and the relative velocity to the gaseous oxygen stream (which was held in constant pressure) decreases, and thus, the droplet size increases.

The droplet size distribution for fuel pressure of 3 bar at the exit of the atomizer and the 60-cm tube is shown in Fig. 6. At the exit of the 60-cm tube, the droplet size distribution shifted toward a larger droplets diameter compared to the distribution at the atomizer exit. The result could have been due to droplet coalescence. Another possible explanation for that could be the diverging spray that has formed a film on the inner wall, and the larger droplets are a result of a wall film breakup. At the tube exit, the measured SMD at equivalence ratio $\phi \approx 1$, for a fuel pressure of 3 bar, is nearly 120 μm, about four times larger than at the atomizer exit. The increase in the size of the droplets due to the tube confinement is similar for fuel pressure of 1.5 bar, as the SMD increased from approximately 25 μm in open space to 110 μm at the tube exit.

Previous studies [5–9] have shown that droplet size below 20 μm led to detonation velocities close to the CJ values and droplet size of about 400 μm led to detonation velocities lower than the CJ values. The effect of change in the droplet size distribution with the fuel flow rate was taken into consideration when analyzing the detonation velocities.

## 2.2 DDT enhancement methods

In addition to the clean configuration engine, some conventional DDT enhancement methods were studied. Shchelkin spirals and a grooved insert were 3D-printed from titanium to resist the engine's severe condition. The Shchelkin spiral had a wire thickness of 1.5 mm, with a pitch of 7 mm and a blockage ratio (BR) of 53%. It had four different lengths of 150, 200, 250, and 300 mm. The grooved insert, as shown in Fig. 8, had a groove depth of 1.5 mm, with a pitch of 10 mm, a blockage ratio of 51%, and a length of 150 mm. All the DDT enhancement methods were tested with the 10-mm-inner-diameter pulse detonation engine. The blockage ratio was based on other studies that concluded that BR between 0.3 and 0.6 was found to provide optimum levels of flame stretching [1,18,19].
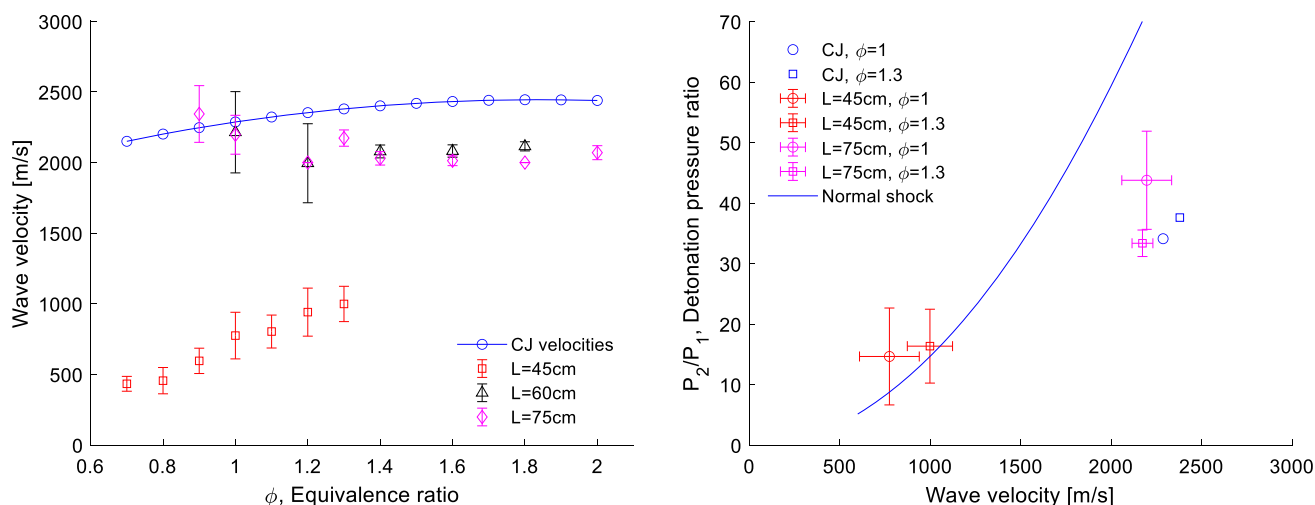
**Fig. 11** Wave velocity (left) and detonation pressure ratio (right) for various engine lengths with an inner diameter $D = 10$ mm
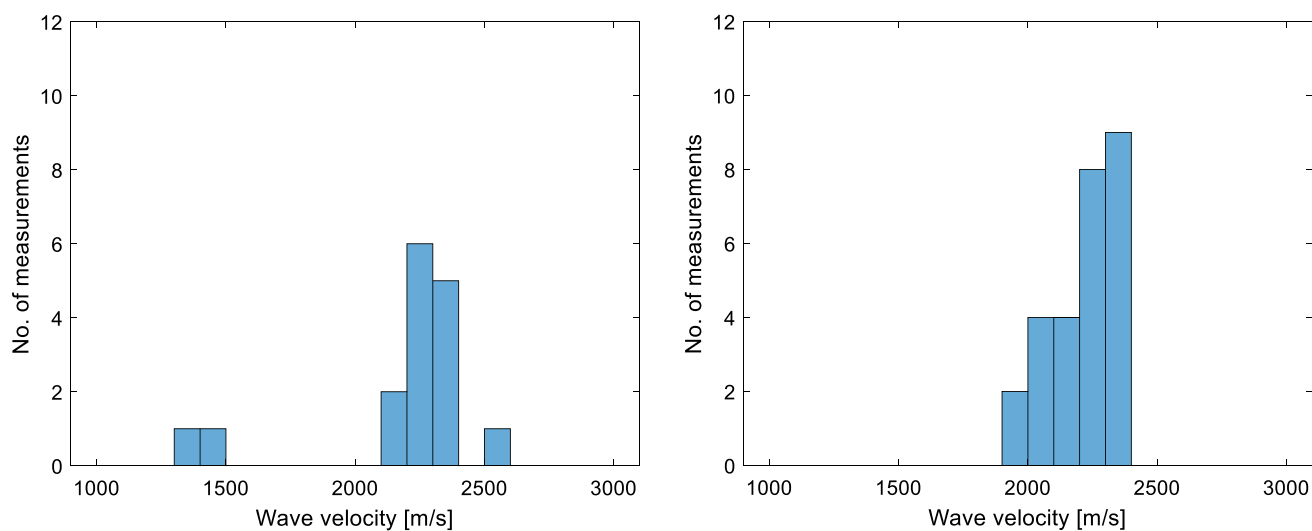


**Fig. 12** Wave velocity histogram for engine length $L = 60$ cm (left) and $L = 75$ cm (right) with an inner diameter $D = 10$ mm and $\phi = 1$

## 2.3 Uncertainty analysis

The reported measurement uncertainties are 0.2% of reading plus 6 g/h for the fuel flow meter (accumulated uncertainty of $\approx 0.3\%$), 0.4% of reading plus 0.2% of full scale for the oxygen flow meter (accumulated uncertainty of $\approx 0.9\%$), 0.1 kPa for the piezoelectric pressure transducers, and 1 μs for the time of arrival. The tolerance of the distance between pressure transducers is less than 0.1 mm. The overall measurement errors are 5% for the velocity and 1.9% for the equivalence ratio. Accumulation of fuel over the wall because of the diverging spray toward the inner tube wall can lead to an error in the measured equivalence ratio of the mixture. The actual equivalence ratio could be leaner than the one reported herein.

## 3 Results and discussion

The experiments showed a consistent detonation with liquid ethanol fuel and oxygen, mainly at fuel-rich mixtures ($0.9 < \phi < 1.8$). Figure 9 shows a typical pressure waveform of a detonation wave, and a detailed pressure trace is shown in Fig. 10. The von Neumann pressure spike is well seen, followed by the Chapman–Jouguet detonation pressure. Pressure traces were used to compute the detonation velocity by measuring time differences of the propagating pressure spike between the two pressure transducers.
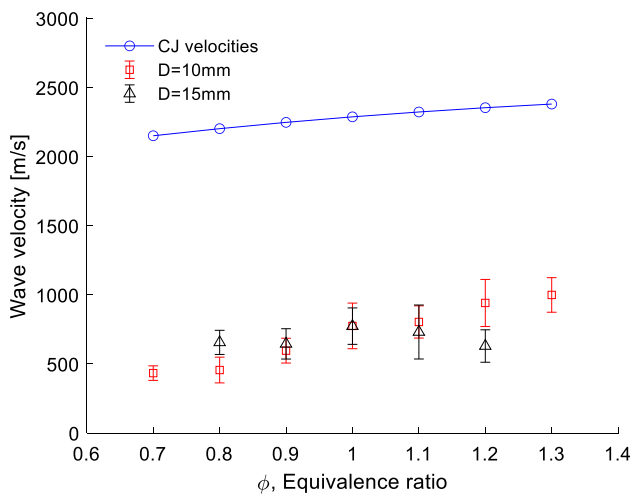
### 3.1 Effects of engine length

The measured detonation velocities for different engine lengths with an inner diameter of 10 mm are shown in Fig. 11
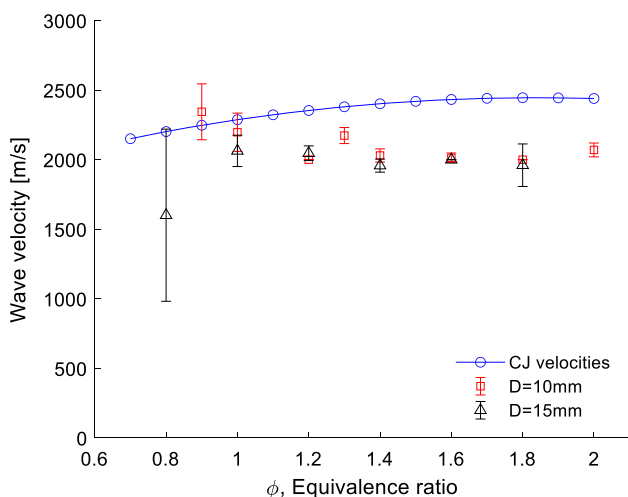
**Fig. 13** Detonation wave velocity for various engine inner diameters and $L = 75$ cm



**Fig. 14** Detonation wave velocity for various engine inner diameters and $L = 45$ cm

(left side). All experimentally reported values for detonation velocity are averages of multiple runs (at least nine measurements) at the same conditions, and the bars represent the standard deviation. The theoretical detonation velocity for the gaseous ethanol–oxygen mixture is shown for a range of equivalence ratios. The distribution of the measured detonation velocities for all runs at equivalence ratio $\phi = 1$ is shown in Fig. 12. Although wide standard deviation exists, most of the measurements are located near the theoretical value.

A gradually increasing wave velocity with equivalence ratio was measured within an engine length of 45 cm. The detonation was not fully developed, and that can explain the lower wave velocities: 470 m/s for $\phi = 0.7$ and 1030 m/s for $\phi = 1.3$. A wave velocity of roughly 2000 m/s was measured within engine lengths of 60 cm and 75 cm. No major differences with equivalence ratio were observed; however,

the measured wave velocities were below theoretical values, as expected for heterogeneous mixture [5–7], mainly for fuel-rich mixtures.

A maximum velocity deficit of approximately 400 m/s was measured for $\phi > 1$, and 100 m/s for $\phi \leq 1$ (within the uncertainty of detonation wave velocity measurement). We assume that it is related to the ethanol droplet size. As shown in Fig. 7, at a higher equivalence ratio, the droplet size distribution shifts toward a larger diameter and result in a less homogeneous mixture that is characterized by a lower evaporation rate and thereby a higher velocity deficit relative to the theoretical gaseous mixture detonation velocity. The same observation was reported by others [5–7].

Due to some accumulation of fuel over the walls, or wall wetting, it is expected that the actual equivalence ratio of the mixture would be slightly lower. A lower equivalence ratio due to wall wetting should be translated to lower CJ velocity. However, at $\phi \leq 1$ the measured wave velocity is very close to the CJ velocity, within the measurement uncertainty, as seen in Fig. 11. Hence, there is no reason to assume that for stoichiometric or lean mixture there was significant wetting on the tube walls. Furthermore, it can be seen in Fig. 11 that for $\phi \geq 1.2$ the measured detonation wave velocity has a very low sensitivity to the equivalence ratio. In addition, the change in the CJ velocity for $\phi \geq 1.2$ is very moderate. Hence, it is not reasonable to attribute the velocity deficit observed for $\phi \geq 1.2$ to a lower apparent equivalence ratio due to wall wetting. It can be concluded that the main reason for the velocity deficit for fuel-rich conditions is the larger fuel droplet size.
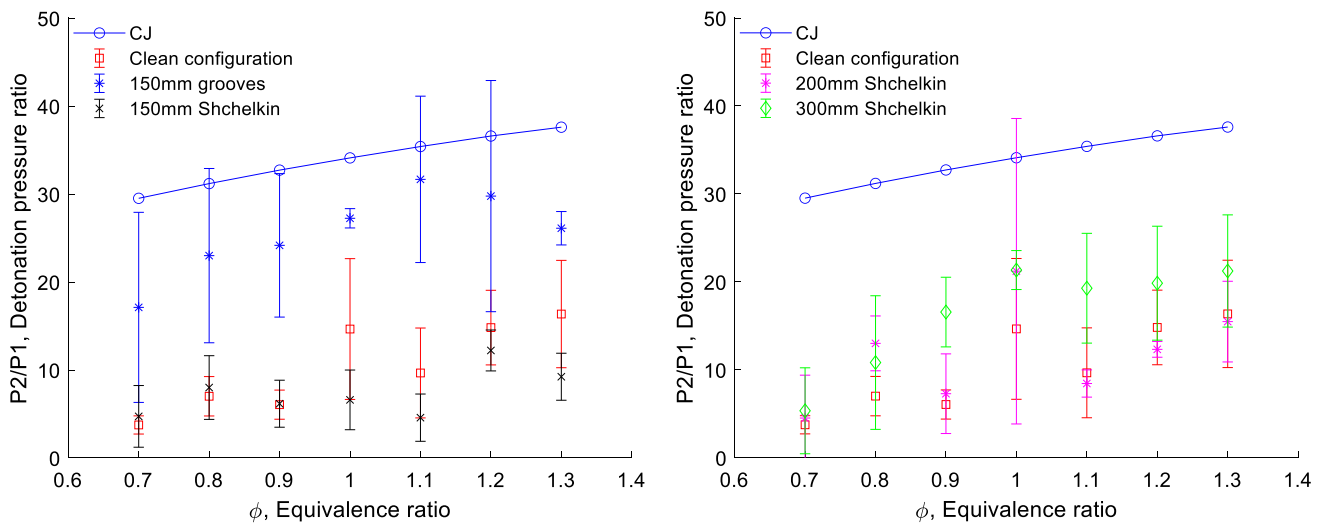
The measured detonation pressure ratios for different engine lengths with an inner diameter of 10 mm and equivalence ratios $\phi = 1$ and $\phi = 1.3$ are shown in Fig. 11 (right). The theoretical detonation pressure ratio for the gaseous ethanol–oxygen mixture is shown for the same equivalence ratios. The detonation pressure ratio should be bounded by an upper limit of the theoretical pressure ratio of a normal shock wave. These values are shown as well. The averages values of pressure ratio are lower for the 45-cm engine length because the detonation was not fully developed, and it increases with length. The measured detonation pressure ratios for engine length of 75 cm are $P_2/P_1 = 43$ for $\phi = 1$ and $P_2/P_1 = 33$ for $\phi = 1.3$. Once again, the heterogeneous nature of the mixture resulted in a lower pressure ratio for fuel-rich mixtures. This fits the lower wave velocity at higher equivalence ratios, and it is expected to be related to larger fuel droplets.

### 3.2 Effects of engine inner diameter

The detonation was considered as fully developed for an engine length of 75 cm; therefore, that was the length selected to study the effects of engine inner diameter. Figure 13 shows the measured detonation velocities for different engine
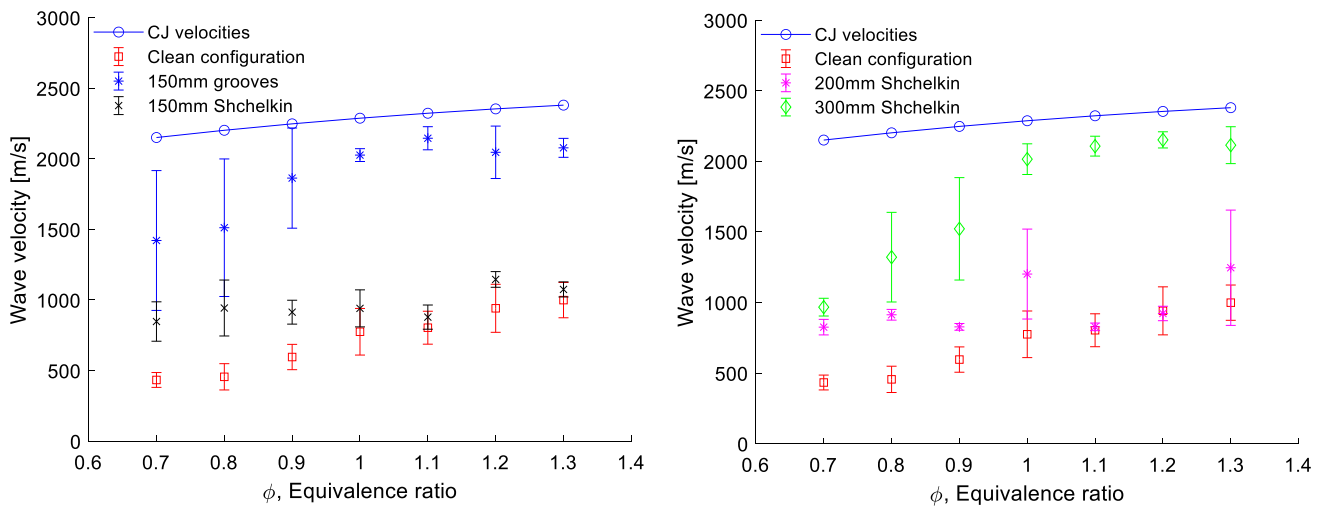
**Fig. 15** Detonation wave velocity for 150-mm Shchelkin spiral and a grooved insert (left) and for 200- and 300-mm Shchelkin spirals (right) with an inner diameter $D = 10$ mm and $L = 45$ cm



**Fig. 16** Detonation wave pressure ratio for 150-mm Shchelkin spiral and a grooved insert (left) and for 200- and 300-mm Shchelkin spirals (right) with an inner diameter $D = 10$ mm and $L = 45$ cm

inner diameters. No significant differences were measured for inner diameters of 10 mm and 15 mm. The wider standard deviation, as seen for $\phi = 0.8$, indicates the mixture's marginal detonability. In this equivalence ratio, some tests developed to detonation, and others did not. The same comparison was made for an engine length of 45 cm to study the effects of inner diameter on the development of detonation. Results are shown in Fig. 14, and there are no significant differences. No detonations were observed for an inner diameter of 6 mm, and we assume that it is related to the cell size of the heterogeneous mixture, which is of the same order as the tube diameter [12–14,20].

## 3.3 Effects of DDT enhancement methods

As described earlier, the 45-cm-long engine was too short for a fully developed detonation with a smooth tube. For that reason, the effect of DDT enhancement methods was tested within that engine length ($L = 45$ cm). The measured results for the clean configuration, without any enhancement methods, were used as a reference for evaluation. A comparison of the measured wave velocities for Shchelkin spirals of different lengths and the grooved insert was made, and the results are shown in Fig. 15. The theoretical detonation velocity for the gaseous ethanol–oxygen mixture is shown

for a range of equivalence ratios. There is an improvement of wave velocity (between 200 and 1000 m/s) with a Shchelkin spiral length of 300 mm, and the trend of rising wave velocity with equivalence ratio is kept. Moreover, there is a significant improvement of the wave velocity with a grooved insert relative to the clean configuration and to the Shchelkin spiral of the same length. For equivalence ratios $\phi \geq 1$, a fully developed detonation has been measured.

As for the pressure ratio behavior, as shown in Fig. 16, shorter spiral (150 mm) results in a lower pressure ratio compared to the clean configuration due to pressure loss because of drag. However, longer spiral (300 mm) that results in a higher pressure ratio suggests a successful coupling of the flame and shock fronts to produce a detonation wave [18], but still not fully developed due to the relatively low wave velocity and pressure ratio. The grooved insert exhibits an improved pressure ratio relative to other Shchelkin spirals and closer to the theoretical detonation pressure ratio.

## 4 Conclusions

An experimental study of a pulse detonation engine with liquid ethanol fuel and oxygen mixture was carried out. Single-cycle tests were made with a modular pulse detonation engine, with several engine lengths and diameters, a variety of equivalence ratios, and different DDT enhancement methods. The ethanol droplet size distribution was measured, and the heterogeneous stoichiometric mixture had an SMD of 30 µm at the exit of the atomizer and an SMD of 120 µm at the nozzle exit. The mixture's initial conditions were 298 K and 101 kPa. A fully developed detonation was observed at and above 60-cm-long smooth tube. A maximum velocity deficit of 400 m/s relative to the theoretical CJ detonation velocity was measured. A weak ignition source of 1.1 mJ and DDT enhancements methods were demonstrated. An improvement of up to 1000 m/s to wave velocity was measured with a Shchelkin spiral and a grooved insert. A longer spiral (200 mm and above) resulted in a higher wave velocity and pressure ratio, probably because of a successful coupling of the flame and shock fronts to produce a detonation wave. The grooved insert exhibits a remarkable improvement relative to other Shchelkin spirals. A 15-cm grooved insert enabled a decrease in the required detonation tube length from 60 to 45 cm, whereas the Shchelkin spiral showed a significantly lower effect. Additional study of the detailed deflagration-to-detonation transition and the ZND reaction zone structure is required.

## References

1. Kailasanath, K.: Recent developments in the research on pulse detonation engines. AIAA J. **41**(2), 145–159 (2003). https://doi.org/10.2514/2.1933
2. Heiser, W.H., David, T.P.: Thermodynamic cycle analysis of pulse detonation engines. J. Propul. Power **18**(1), 68–76 (2002). https://doi.org/10.2514/2.5899
3. Roy, G.D., Frolov, S.M., Borisov, A.A., Netzer, D.W.: Pulse detonation propulsion: challenges, current status, and future perspective. Prog. Energy Combust. Sci. **30**(6), 545–672 (2004). https://doi.org/10.1016/j.pecs.2004.05.001
4. Kailasanath, K.: Liquid-fueled detonations in tubes. J. Propul. Power **22**(6), 1261–1268 (2006). https://doi.org/10.2514/1.19624
5. Dabora, E.K., Ragland, K.W., Nicholls, J.A.: A study of heterogeneous detonations. 3rd Aerospace Sciences Meeting, New York, NY, AIAA Paper 1966-109 (1966). https://doi.org/10.2514/6.1966-109
6. Dabora, E.K., Weinberger, L.P.: Present status of detonations in two-phase systems. Acta Astronaut. **1**(3–4), 361–372 (1974). https://doi.org/10.1016/0094-5765(74)90103-9
7. Gubin, S.A., Sichel, M.: Calculation of the detonation velocity of a mixture of liquid fuel droplets and a gaseous oxidizer. Combust. Sci. Technol. **17**(3–4), 109–117 (1977). https://doi.org/10.1080/00102207708946821
8. Brophy, C.M., Netzer, D.W., Forster, D.: Detonation studies of JP-10 with oxygen and air for pulse detonation engine development. 34th AIAA/ASME/SAE/ASEE Joint Propulsion Conference and Exhibit, Cleveland, OH, AIAA Paper 1998-4003 (1998). https://doi.org/10.2514/6.1998-4003
9. Brophy, C.M., Netzer, D.W., Sinibaldi, J., Johnson, R.: Detonation of a JP-10 aerosol for pulse detonation applications. High-Speed Deflagration and Detonation, pp. 207–222. Elex-KM Publ., Moscow (2001)
10. Frolov, S.M., Basevich, V.Y., Aksenov, V.S., Polikhov, S.A.: Optimization study of spray detonation initiation by electric discharges. Shock Waves **14**(3), 175–186 (2005). https://doi.org/10.1007/s00193-005-0263-8
11. Bar-Or, R., Sichel, M., Nicholls, J.A.: The propagation of cylindrical detonations in monodisperse sprays. Symp. (Int.) Combust. **18**(1), 1599–1606 (1981). https://doi.org/10.1016/S0082-0784(81)80163-4
12. Diakow, P., Cross, M., Ciccarelli, G.: Detonation characteristics of dimethyl ether and ethanol-air mixtures. Shock Waves **25**(3), 231–238 (2015). https://doi.org/10.1007/s00193-015-0554-7
13. Mendiburu Zevallos, A.A., Ciccarelli, G., Carvalho Jr., J.L.: DDT limits of ethanol-air in an obstacles-filled tube. Combust. Sci. Technol., pp. 1–16 (2018). https://doi.org/10.1080/00102202.2018.1477770
14. Ng, H.D., Chao, J., Yatsufusa, T., Lee, J.H.: Measurement and chemical kinetic prediction of detonation sensitivity and cellular structure characteristics in dimethyl ether-oxygen mixtures. Fuel **88**(1), 124–131 (2009). https://doi.org/10.1016/j.fuel.2008.07.029
15. Ng, H.D., Yiguang, J., Lee, J.H.: Assessment of detonation hazards in high-pressure hydrogen storage from chemical sensitivity analysis. Int. J. Hydrog. Energy **32**(1), 93–99 (2007). https://doi.org/10.1016/j.ijhydene.2006.03.012
16. Eaton, R., Zhang, B., Bergthorson, J.M., Ng, H.D.: Measurement and chemical kinetic model predictions of detonation cell size in methanol-oxygen mixtures. Shock Waves **22**(2), 173–178 (2012). https://doi.org/10.1007/s00193-012-0359-x
17. Panicker, P., Wilson, D., Lu, F.: Operational issues affecting the practical implementation of pulse detonation engines. 14th AIAA/AHI Space Planes and Hypersonic Systems and Technolo-

gies Conference, Canberra, Australia, AIAA Paper 2006-7959 (2006). https://doi.org/10.2514/6.2006-7959

18. New, T., Panicker, P., Lu, F., Tsai, H.: Experimental investigations on DDT enhancements by Shchelkin spirals in a PDE. 44th AIAA Aerospace Sciences Meeting and Exhibit, Reno, NV, AIAA Paper 2006-552 (2006). https://doi.org/10.2514/6.2006-552

19. New, T., Panicker, P., Chui, K., Tsai, H., Lu, F.: Experimental study on deflagration-to-detonation transition enhancement methods in a PDE. 14th AIAA/AHI Space Planes and Hypersonic Systems and Technologies Conference, Canberra, Australia, AIAA Paper 2006-7958 (2006). https://doi.org/10.2514/6.2006-7958

20. Kadosh, H., Michaels, D.: Measurement of detonation cell size in liquid ethanol and oxygen mixtures. Shock Waves (2021). https://doi.org/10.1007/s00193-021-01064-0